Kerr-lens mode-locked Tm-doped sesquioxide ceramic laser

Yongguang Zhao, Li Wang, Weidong Chen, Pavel Loiko, Yicheng Wang, Zhongben Pan, Hanlin Yang, Wei Jing, Hui Huang, Jiachen Liu, et al.

Kerr-lens mode-locked Tm-doped sesquioxide ceramic laser

YONGGUANG ZHAO,[1,2] LI WANG,[1] WEIDONG CHEN,[1,3,*] PAVEL LOIKO,[4] YICHENG WANG,[1,5] ZHONGBEN PAN,[6] HANLIN YANG,[6,7] WEI JING,[6] HUI HUANG,[6] JIACHEN LIU,[7] XAVIER MATEOS,[8,#] ZHENGPING WANG,[9] XINGUANG XU,[9] UWE GRIEBNER,[1] AND VALENTIN PETROV[1]

[1]*Max Born Institute for Nonlinear Optics and Short Pulse Spectroscopy, Max-Born-Str. 2a, 12489 Berlin, Germany*
[2]*Jiangsu Key Laboratory of Advanced Laser Materials and Devices, Jiangsu Normal University, Xuzhou 221116, China*
[3]*Key Laboratory of Optoelectronic Materials Chemistry and Physics, Fujian Institute of Research on the Structure of Matter, Chinese Academy of Sciences, Fuzhou, 350002 Fujian, China*
[4]*Centre de Recherche sur les Ions, les Matériaux et la Photonique (CIMAP), UMR 6252 CEA-CNRS-ENSICAEN, Université de Caen, 6 Boulevard du Maréchal Juin, 14050 Caen Cedex 4, France*
[5]*Photonics and Ultrafast Laser Science, Ruhr Universität Bochum, Universitätsstraße 150, 44801 Bochum, Germany*
[6]*Institute of Chemical Materials, China Academy of Engineering Physics, Mianyang 621900, China*
[7]*Key Laboratory of Advanced Ceramics and Mechanical Technology of Ministry of Education, School of Materials Science and Engineering, Tianjin University, Tianjin 300072, China*
[8]*Universitat Rovira i Virgili, Física i Cristal·lografia de Materials i Nanomaterials (FiCMA-FiCNA) 43007, Tarragona, Spain. #Serra Húnter Fellow*
[9]*State Key Laboratory of Crystal Materials and Institute of Crystal Materials, Shandong University, Jinan 250100, China*
**Corresponding author: Weidong.Chen@mbi-berlin.de*

Received XX Month XXXX; revised XX Month, XXXX; accepted XX Month XXXX; posted XX Month XXXX (Doc. ID XXXXX); published XX Month XXXX

Kerr-lens mode-locked solid-state laser operation at ~ 2 µm is investigated. Using a Tm^{3+}-doped $(Lu,Sc)_2O_3$ "mixed" sesquioxide ceramic as a gain medium, pulses as short as 58 fs are generated at ~2081 nm via soft-aperture Kerr-lens mode-locking. The average output power amounts to 220 mW at a pulse repetition rate of 84.8 MHz. The emitted spectrum at the long-wavelength wing extends to > 2.2 µm which is attributed to vibronic transitions of the Tm^{3+} ions. The latter is found to be essential for generating pulses with durations in the 50-fs range.

http://dx.doi.org/10.1364/OL.99.099999

Since the first demonstration of sub-100 fs bulk lasers emitting in the 2 µm spectral range in 2017, a Tm:$MgWO_4$ laser mode-locked (ML) by graphene saturable absorber (SA) [1], a remarkable progress has been achieved in this field. Several types of "slow" SAs, such as SEmiconductor Saturable Absorber Mirrors (SESAMs) [2] and single-walled carbon nanotubes (SWCNTs) [3, 4] were applied to start and stabilize the soliton type mode-locking [5]. Pulses as short as 54 fs at 2048 nm were generated from a SESAM ML Tm:$(Lu,Y)_2O_3$ "mixed" ceramic laser with an average output power of 51 mW [6]. A slightly longer pulse duration of 57 fs was reported using the same gain material and a SWCNT-SA [7].

Kerr-lens mode-locking (KLM) is another, well-established technique, in particular interesting for the 2-µm spectral range where no commercially available SAs exist. It is based on self-focusing in combination with an intracavity aperture. This creates an intensity dependent quasi-instantaneous self-amplitude modulation which acts as an artificial "fast" SA supporting the generation of extremely short pulses down to few fs [8, 9]. KLM features: (i) support of broadband operation without the penalty of the non-saturable loss of "slow" SAs [10], and (ii) no operating wavelength limitations inherent to "slow" SAs [11, 12].

The challenge of KLM near 2 µm as compared to 1-µm relates to a great extent to the weaker Kerr effect (lower nonlinear refractive index (n_2) for a given laser host material) and the associated higher critical power for self-focusing. Normally, tight focusing in the laser gain medium or an extra Kerr material is required to overcome the above-mentioned limitations. Nevertheless the first KLM laser around 2 µm was demonstrated only in 2017 [13-15], 8 years after the first passively ML laser using a "slow" SA [16]. The first sub-100-fs KLM Tm laser comprised a Tm:Sc_2O_3 crystal pumped by a 1611 nm fiber amplifier. It delivered 72-fs pulses at 2108 nm with an average output power of 130 mW [17]. Subsequently, a "slow" SWCNT-SA-assisted KLM operation was also demonstrated and 76-fs were generated at 2037 nm from a Tm:$MgWO_4$ laser [18].

Compared to other Tm^{3+} laser host materials, the cubic sesquioxides A_2O_3 (where A = Y, Lu, Sc or their combination) exhibit a relatively high n_2 value favoring KLM operation. Their

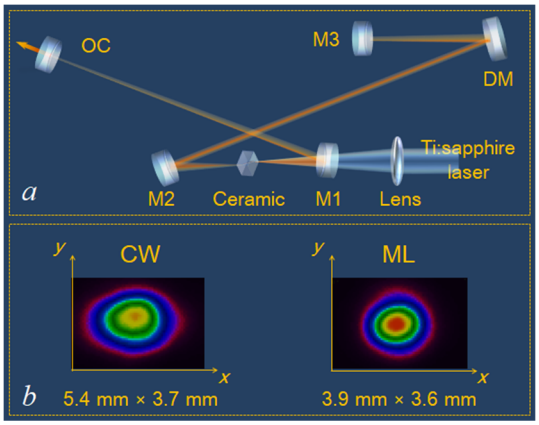

Fig. 1. Schematic of the KLM Tm:$(Lu,Sc)_2O_3$ ceramic laser (a). Output beam profiles in the CW and ML regimes (b). (M1-M2, dichroic mirrors; DM, dispersive mirror; OC, output coupler; CW, continuous wave; ML, mode-locked).

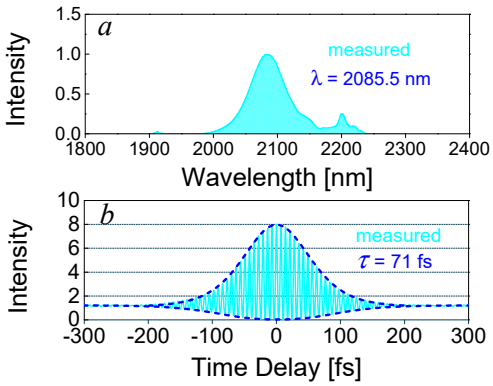

Fig. 2. KLM Tm:$(Lu,Sc)_2O_3$ ceramic laser with T_{OC} = 0.5%. Optical spectrum (a) and interferometric autocorrelation trace (b).

strong crystal field and large ground-state Stark splitting lead to smooth and broad gain profiles supporting emission far beyond 2 µm, which is exceptional among the Tm^{3+}-doped materials. Furthermore, their attractive thermo-mechanical properties favor high average/peak power ML operation [19].

The technology of transparent polycrystalline ceramics not only relaxes the constraint of high melting temperatures for the sesquioxides, but also offers easier elaboration of "mixed"materials which exhibit compositional disorder leading to additional inhomogeneous broadening of the dopant spectral lines. Here, based on the extremely smooth and broad gain profiles of Tm^{3+}-doped "mixed" lutetia-scandia $(Lu,Sc)_2O_3$ transparent ceramics in conjunction with their relatively large n_2 value we explore the power scalability of sub-100-fs KLM lasers at ~ 2 µm.

Almost pore-free Tm:$(Lu_{2/3}Sc_{1/3})_2O_3$ transparent ceramic with a measured Tm^{3+} doping level of 2.8 at.% was fabricated by Hot Isostatic Pressing (HIP) of commercial powders at 1800°C/195 MPa in Ar atmosphere [20]. KLM laser operation was investigated using a five-mirror linear astigmatically compensated X-shaped cavity. The uncoated ceramic sample with an aperture of 3 mm × 3 mm and a thickness of 3 mm was mounted in a water-cooled copper holder (coolant temperature: 14°C) and placed at Brewster's angle between two concave dichroic folding mirrors M1 and M2 (RoC = -100 mm). A 795 nm narrow-linewidth continuous-wave (CW) Ti:Sapphire laser was used as a pump source. The pump beam was focused into the ceramic sample by a spherical lens (f = 70 mm) resulting in a beam waist radius of 33 µm × 77 µm in the sagittal and tangential planes, respectively. The corresponding cavity waist radius in the CW mode inside the ceramic sample, estimated by the ABCD formalism, was 30 µm × 57 µm. The cavity was completed by a flat dispersive mirror (DM), a flat rear mirror (M3), and a plane-wedged output coupler (OC), Fig. 1(a). The roundtrip group delay dispersion (GDD) due to the 3-mm thick ceramic sample amounted to -200 fs^2 at 2.08 µm, estimated by averaging the refractive indices of Lu_2O_3 and Sc_2O_3 [21]. Taking into account the GDD of the bending DM (~ –800 fs^2 per bounce in the spectral range from 2.0 to 2.2 µm) the total round-trip GDD amounted to ~–1850 fs^2.

The Tm:$(Lu,Sc)_2O_3$ ceramic laser was initially characterized in the CW regime with a 0.5% OC. At an absorbed pump power (P_{abs}) of 1.8 W, a maximum CW output power of 490 mW was achieved at 2088.1 nm with an optical conversion efficiency of 26.8%. KLM operation was established by aligning the resonator towards the edge of the stability region by translating the folding mirror (M2) by several hundreds of micrometers away from the pump mirror (M1) to discriminate the CW regime. KLM was not self-starting. The transition from the CW to the KLM regime was achieved by a slight knock on the flat rear mirror (M3) or the OC. This led to abrupt increase in the average output power from 147 to 247 mW. At P_{abs} = 1.1 W the corresponding optical conversion efficiency was 22.5%. Figure 2 shows the recorded optical spectrum and the interferometric autocorrelation trace. The spectrum was centered at 2085.5 nm with a full width at half maximum (FWHM) of 65 nm, Fig. 2(a). The autocorrelation trace gives a pulse duration of 71 fs by assuming a $sech^2$-shaped temporal profile, see Fig. 2(b), which is 22.4% longer than the Fourier-transform limit. A significant change in the recorded far-field beam profile was observed by placing an infrared camera at ~2 m from the OC. The shrinking of the far-field beam diameter from 5.4 (x) mm × 3.7 (y) mm to 3.9 (x) mm × 3.6 (y) mm, as shown in Fig. 1(b), is a clear evidence for a soft-aperture Kerr-lens effect and self-focusing inside the ceramic sample. The total cavity length was ~ 1.8 m resulting in a pulse repetition rate of ~84.8 MHz. The peak on-axis laser intensity in the ceramic was estimated to be ~510 GW/cm^2.

The pulse duration was further shortened by using a 0.2% OC while maintaining P_{abs} = 1.1 W. The average output power dropped to 136 mW, however, the FWHM of the spectrum increased to 70 nm. Scaling of the pump power while maintaining the soft-aperture KLM regime, was possible up to P_{abs} = 1.6 W resulting in an average output power of 220 mW. The optical spectrum was further broadened but exhibited a significant deviation from an ideal $sech^2$-shape profile, with three distinct peaks at 2081.4, 2181.5 and 2226.7 nm, see Fig. 3(a). Pulses as short as 58 fs were recorded after external linear chirp compensation with a 3-mm thick ZnS ceramic plate (GDD = 465 fs^2). This pulse duration is equivalent to 8 optical cycles which was confirmed by recording the fringe-resolved autocorrelation trace, presented in Fig. 3(b). A long-scale intensity autocorrelation scan (15 ps) is shown in the inset of Fig 3(b), confirming a single pulse ML operation without any pedestals or multi-pulses. The deconvolved pulse duration was 13.7% above the Fourier-transform limit, see Fig. 3(a). The peak on-axis laser intensity in the ceramic was ~623 GW/cm^2. Compared to previous sub-100 fs pulse generation results obtained with Tm-doped mixed sesquioxide ceramics using real SAs [2, 6, 7], KLM clearly demonstrates average power scalability

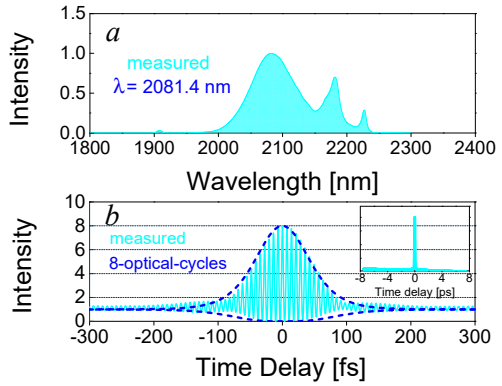

Fig. 3. KLM Tm:$(Lu,Sc)_2O_3$ ceramic laser with $T_{OC} = 0.2\%$. Optical spectrum (a) and interferometric autocorrelation traces of the shortest pulses (b). *Inset* in (b): simultaneously measured long-scale (±7.5 ps) background- free autocorrelation trace.

combined with shortest pulse durations.

The KLM pulse train was characterized by a radio frequency (RF) spectrum analyzer. The recorded fundamental beat note at 84.8 MHz exhibited a high extinction ratio of 77 dBc above the noise level, see Fig. 4(a). This, together with the uniform harmonic beat notes shown in Fig 4(b) indicates highly stable ML operation without any unwanted Q-switched or multiple pulsing instabilities.

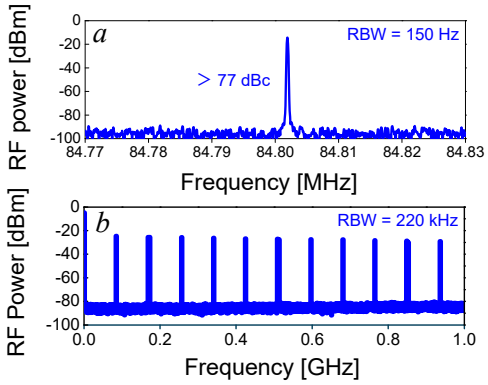

Fig. 4. RF spectra of the KLM Tm:$(Lu,Sc)_2O_3$ ceramic laser: fundamental beat note (a) and 1-GHz span (b). RBW: resolution bandwidth.

For sub-80 fs pulses, the broadband long-wavelength emission extended to ~2.2 μm, see Fig. 2(a) and Fig. 3(a). Given a strong coupling between the electronic transition of Tm^{3+} ions and the host material phonons exists, this emission may refer to multiphonon-assisted transitions of the Tm^{3+} ions [22, 23]. To confirm this hypothesis, we calculated the stimulated emission (SE) cross-section spectrum for the $^3F_4 \rightarrow {}^3H_6$ transition of Tm^{3+} ions in the Tm:$(Lu,Sc)_2O_3$ ceramic, see Fig. 5(a). According to the Stark splitting of the $^3H_6$ and $^3F_4$ Tm^{3+} multiplets determined at 10 K, the purely electronic transitions at room temperature (RT) were computed as shown by vertical dashes in Fig. 5(a).

Among them, the longest wavelength is 2099 nm which corresponds to an electronic transition occurring from the lowest Stark level (sub-level) of the $^3F_4$ multiplet (5683 cm^{-1}) to the highest sub-level of the $^3H_6$ multiplet (919 cm^{-1}). The emission at longer wavelengths extending up to 2.3 μm has a vibronic nature

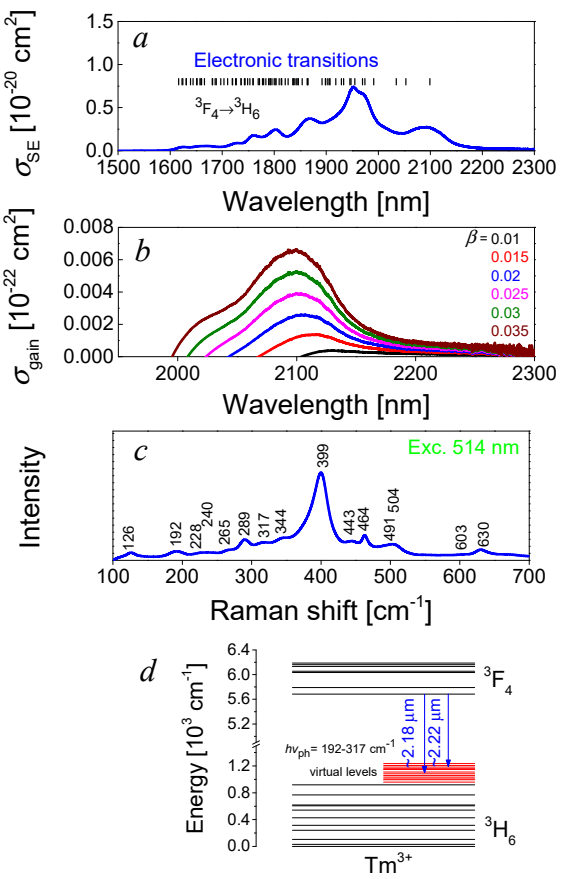

Fig. 5. Spectroscopy of Tm:$(Lu,Sc)_2O_3$ ceramic: (a) stimulated-emission cross-section, σ_{SE}, for the $^3F_4 \rightarrow {}^3H_6$ transition, vertical dashes mark all possible wavelengths of purely electronic Stark transitions, (b) calculated gain cross-section, σ_{gain}, spectra for different inversion rates $\beta = N_2(^3F_4)/N_{Tm}$, (c) Raman spectrum, $\lambda_{exc} = 514$ nm, *numbers* denote the peak frequencies in cm^{-1}; (d) Derived crystal-field splitting of $^3H_6$ and $^3F_4$ multiplets of Tm^{3+} ions in C_2 sites revealed at 10 K. The red lines illustrate virtual energy-levels due to electron-phonon coupling with the host vibrations participating in laser emission at ~2.1 - 2.2 μm.

and it determines to a large extent the gain spectra for small inversion rates β, see Fig. 5(b). For very small inversion rates (high finesse cavities), e.g., $\beta = 0.01$, the gain cross-section spectrum reveals a smooth and broad profile from 2.1 to 2.3 μm. For slightly higher β, a local peak at ~2.1 μm emerges, spanning from ~2.0 to 2.3 μm, in agreement with our observations in the present KLM Tm:$(Lu,Sc)_2O_3$ ceramic laser, cf. Fig. 2(a) and Fig. 3(a).

The measured Raman spectrum of the Tm:$(Lu,Sc)_2O_3$ ceramic is shown in Fig. 5(c). Apart from the most intense band at 399 cm^{-1}, it reveals multiple bands at lower frequencies, 126-344 cm^{-1}. By adding these vibrations to the higher-lying sub-levels of the $^3H_6$ ground state (representing an electron-phonon coupling), we obtain a set of densely located virtual energy levels at 768 - 1236 cm^{-1}, as shown in Fig. 5(d). The long-wave emission above 2.1 μm can be thus explained by transitions from the upper laser level ($^3F_4$) to one or several of such virtual levels (lower laser level). Full utilization of the vibronic emission in the present ML laser is impossible mainly due to the reflectivity characteristics of the pump mirror M1 and the OC. They limit the spectrum from the long wave side starting from ~2.2 μm and prevent operation in the flat gain region, see Fig. 5(b). The spectral and temporal reshaping

of the laser output through the OC in particular results in a significant deviation from the ideal $sech^2$-shape spectral profile indicated by structured satellite peaks around ~2.2 μm, cf. Fig. 2(a) and Fig. 3(a) but also in deviation from the ideal temporal fit, cf. Fig. 3(b). The unmanageable intracavity GDD at the long-wave spectral wing beyond 2.1 μm due to the same cavity elements may also contribute to the formation of such satellites, however the gain at such wavelengths is still provided by vibronic emission. The appearance of such spectral sidebands at the long-wave wing was also observed in other ML Tm-doped sesquioxide lasers when the spectral bandwidths exceeded 60 nm [2, 6, 7, 17]. Alternative gain mechanisms at such long wavelengths suggested in [17] include stimulated Raman scattering and the upper lying $^3H_4 \rightarrow {}^3H_5$ Tm^{3+} transition but we have no evidence for such effects in our laser.

In conclusion, we have demonstrated a KLM Thulium sesquioxide laser based on a "mixed" Tm:$(Lu,Sc)_2O_3$ transparent ceramic. Using a 0.2% OC, pulses as short as 58 fs, i.e., 8 optical cycles, were generated at ~2081 nm. The average output power amounted to 220 mW at a repetition rate of 84.8 MHz. Thus, KLM using other Tm-doped broadband gain media (e.g., disordered or composite ones) and/or a proper cavity design is expected to provide yet shorter pulses near 2 μm, i.e., few optical cycles. The observation of long-wave emission at ~2.2 μm within the ML laser spectrum indicates contribution of Tm^{3+} vibronic transitions. Having in mind that such multiphonon-assisted long wavelength emission can be fully resonated it seems advantageous for further spectral broadening and pulse shortening.

Funding. National Natural Science Foundation of China (52032009, 61975208, 62075090, 51761135115, 61850410533, 52072351); Deutsche Forschungsgemeinschaft (PE 607/14-1); Natural Science Foundation of Jiangsu Province (BK20190104); Sino-German Scientist Cooperation and Exchanges Mobility Programme (M-0040); Foundation of President of China Academy of Engineering Physics (CAEP) (YZJJLX2018005); Fundation of Key Laboratory of Research on Chemistry and Physics of Optoelectronic Materials (CAS 2008DP173016).

Acknowledgment. Y. Zhao acknowledges financial support from the Alexander von Humboldt Foundation through a Humboldt fellowship.

Disclosures. The authors declare no conflicts of interest

Disclosures. Data underlying the results presented in this paper are not publicly available at this time but may be obtained from the authors upon reasonable request.

References

1. Y. C. Wang, W. D. Chen, M. Mero, L. Z. Zhang, H. F. Lin, Z. B. Lin, G. Zhang, F. Rotermund, Y. J. Cho, P. Loiko, X. Mateos, U. Griebner, and V. Petrov, Opt. Lett. **42**, 3076 (2017).
2. Y. Wang, W. Jing, P. Loiko, Y. Zhao, H. Huang, X. Mateos, S. Suomalainen, A. Härkönen, M. Guina, U. Griebner, and V. Petrov, Opt. Express **26**, 10299 (2018).
3. Y. Wang, Y. Zhao, Z. Pan, J. E. Bae, S. Y. Choi, F. Rotermund, P. Loiko, J. M. Serres, X. Mateos, H. Yu, H. Zhang, M. Mero, U. Griebner, and V. Petrov, Opt. Lett. **43**, 4268 (2018).
4. Z. Pan, Y. Wang, Y. Zhao, H. Yuan, X. Dai, H. Cai, J. E. Bae, S. Y. Choi, F. Rotermund, X. Mateos, J. M. Serres, P. Loiko, U. Griebner, and V. Petrov, Photon. Res. **6**, 800 (2018).
5. V. Petrov, Y. Wang, W. Chen, Z. Pan, Y. Zhao, L. Wang, M. Mero, S. Y. Choi, F. Rotermund, W. B. Cho, J. Wei, H. Huang, H. Cai, L. Zhang, Z. Lin, P. Loiko, X. Mateos, X. Xu, J. Xu, H. Yu, H. Zhang, S. Suomalainen, M. Guina, A. Härkönen and U. Griebner, Proc. SPIE **11209**, 112094G (2020).
6. Y. Zhao, L. Wang, W. Chen, Z. Pan, Y. Wang, P. Liu, X. Xu, Y. Liu, D. Shen, J. Zhang, M. Guina, X. Mateos, P. Loiko, Z. Wang, X. Xu, J. Xu, M. Mero, U. Griebner, and V. Petrov, Appl. Opt. **59**, 10493 (2020).
7. Y. Zhao, L. Wang, Y. Wang, J. Zhang, P. Liu, X. Xu, Y. Liu, D. Shen, J. E. Bae, T. G. Park, F. Rotermund, X. Mateos, P. Loiko, Z. Wang, X. Xu, J. Xu, M. Mero, U. Griebner, V. Petrov, and W. Chen, Opt. Lett. **45**, 459 (2020).
8. T. Brabec, C. Spielmann, P. F. Curley, and F. Krausz, Opt. Lett. **17**, 1292 (1992).
9. R. Ell, U. Morgner, F. X. Kärtner, J. G. Fujimoto, E. P. Ippen, V. Scheuer, G. Angelow, T. Tschudi, M. J. Lederer, and A. Boiko, Opt. Lett. **26**, 373 (2001).
10. O. Pronin, and J. Brons, in *High Power Laser Systems* (IntechOpen, 2018).
11. S. Ruan, J. M. Sutherland, P. M. W. French, J. R. Taylor, and B. H. T. Chai, Opt. Lett. **20**, 1041 (1995).
12. R. Paiella, F. Capasso, C. Gmachl, D. L. Sivco, J. N. Baillargeon, A. L. Hutchinson, A. Y. Cho, and H. C. Liu, Science **290**, 1739 (2000).
13. F. Canbaz, I. Yorulmaz, and A. Sennaroglu, Opt. Lett. **42**, 3964 (2017).
14. J. Zhang, K. F. Mak, and O. Pronin, IEEE J. Sel. Top. Quantum Electron. **24**, 1 (2018).
15. M. Tokurakawa, E. Fujita, and C. Kränkel, Opt. Lett. **42**, 3185 (2017).
16. W. B. Cho, A. Schmidt, J. H. Yim, S. Y. Choi, S. Lee, F. Rotermund, U. Griebner, G. Steinmeyer, V. Petrov, X. Mateos, M. C. Pujol, J. J. Carvajal, M. Aguilo, and F. Diaz, Opt. Express **17**, 11007 (2009).
17. A. Suzuki, C. Kränkel, and M. Tokurakawa, Appl. Phys. Express **13**, 052007 (2020).
18. L. Wang, W. Chen, Y. Zhao, Y. Wang, Z. Pan, H. Lin, G. Zhang, L. Zhang, Z. Lin, and J. Bae, T. G. Park, F. Rotermund, P. Loiko, X. Mateos, M. Mero, U. Griebner and V. Petorv, Opt. Lett. **45**, 6142 (2020).
19. C. Kränkel, IEEE J. Sel. Top. Quantum Electron. **21** (2015).
20. W. Jing, P. Loiko, J. M. Serres, Y. Wang, E. Vilejshikova, M. Aguiló, F. Díaz, U. Griebner, H. Huang, V. Petrov, and X. Mateos, Opt. Mater. Express **7**, 4192 (2017).
21. D. E. Zelmon, J. M. Northridge, N. D. Haynes, D. Perlov, and K. Petermann, Appl. Opt. **52**, 3824 (2013).
22. P. Loiko, Y. C. Wang, J. M. Serres, X. Mateos, M. Aguilo, F. Diaz, L. Z. Zhang, Z. B. Lin, H. F. Lin, G. Zhang, E. Vilejshikova, E. Dunina, A. Kornienko, L. Fomicheva, V. Petrov, U. Griebner, and W. D. Chen, J. Alloy Compd. **763**, 581 (2018).
23. P. Loiko, X. Mateos, S. Y. Choi, F. Rotermund, J. M. Serres, M. Aguiló, F. Díaz, K. Yumashev, U. Griebner, and V. Petrov, J. Opt. Soc. Am. B **33**, D19 (2016).

References

1. Y. C. Wang, W. D. Chen, M. Mero, L. Z. Zhang, H. F. Lin, Z. B. Lin, G. Zhang, F. Rotermund, Y. J. Cho, P. Loiko, X. Mateos, U. Griebner, and V. Petrov, "Sub-100 fs Tm:$MgWO_4$ laser at 2017 nm mode locked by a graphene saturable absorber," Optics Letters **42**, 3076-3079 (2017).
2. Y. Wang, W. Jing, P. Loiko, Y. Zhao, H. Huang, X. Mateos, S. Suomalainen, A. Härkönen, M. Guina, U. Griebner, and V. Petrov, "Sub-10 optical-cycle passively mode-locked Tm:$(Lu_{2/3}Sc_{1/3})_2O_3$ ceramic laser at 2 μm," Optics Express **26**, 10299-10304 (2018).
3. Y. Wang, Y. Zhao, Z. Pan, J. E. Bae, S. Y. Choi, F. Rotermund, P. Loiko, J. M. Serres, X. Mateos, H. Yu, H. Zhang, M. Mero, U. Griebner, and V. Petrov, "78 fs SWCNT-SA mode-locked Tm:CLNGG disordered garnet crystal laser at 2017 nm," Optics Letters **43**, 4268-4271 (2018).
4. Z. Pan, Y. Wang, Y. Zhao, H. Yuan, X. Dai, H. Cai, J. E. Bae, S. Y. Choi, F. Rotermund, X. Mateos, J. M. Serres, P. Loiko, U. Griebner, and V. Petrov, "Generation of 84-fs pulses from a mode-locked Tm:CNNGG disordered garnet crystal laser," Photonics Research **6**, 800-804 (2018).
5. V. Petrov, Y. Wang, W. Chen, Z. Pan, Y. Zhao, L. Wang, M. Mero, S. Y. Choi, F. Rotermund, W. B. Cho, W. Jing, H. Huang, H. Yuan, H. Cai, L. Zhang, Z. Lin, P. Loiko, X. Mateos, X. Xu, J. Xu, H. Yu, H. Zhang, S. Suomalainen, M. Guina, A. Härkönen, and U. Griebner, *Sub-100-fs bulk solid-state lasers near 2-micron* (SPIE, 2019).
6. Y. Zhao, L. Wang, W. Chen, Z. Pan, Y. Wang, P. Liu, X. Xu, Y. Liu, D. Shen, J. Zhang, M. Guina, X. Mateos, P. Loiko, Z. Wang, X. Xu, J. Xu, M. Mero, U. Griebner, and V. Petrov, "SESAM mode-locked Tm:$LuYO_3$ ceramic laser generating 54-fs pulses at 2048 nm," Applied Optics **59**, 10493-10497 (2020).
7. Y. Zhao, L. Wang, Y. Wang, J. Zhang, P. Liu, X. Xu, Y. Liu, D. Shen, J. E. Bae, T. G. Park, F. Rotermund, X. Mateos, P. Loiko, Z. Wang, X. Xu, J. Xu, M. Mero, U. Griebner, V. Petrov, and W. Chen, "SWCNT-SA mode-locked Tm:$LuYO_3$ ceramic laser delivering 8-optical-cycle pulses at 2.05 μm," Optics Letters **45**, 459-462 (2020).
8. T. Brabec, C. Spielmann, P. F. Curley, and F. Krausz, "Kerr lens mode locking," Optics Letters **17**, 1292-1294 (1992).
9. R. Ell, U. Morgner, F. X. Kärtner, J. G. Fujimoto, E. P. Ippen, V. Scheuer, G. Angelow, T. Tschudi, M. J. Lederer, and A. Boiko, "Generation of 5-fs pulses and octave-spanning spectra directly from a Ti:sapphire laser," Optics Letters **26**, 373-375 (2001).
10. O. Pronin, and J. Brons, "Kerr-Lens Mode-Locked High-Power Thin-Disk Oscillators," in *High Power Laser Systems*(IntechOpen, 2018).
11. S. Ruan, J. M. Sutherland, P. M. W. French, J. R. Taylor, and B. H. T. Chai, "Kerr-lens mode-locked visible transitions of a Pr:YLF laser," Optics Letters **20**, 1041-1043 (1995).
12. R. Paiella, F. Capasso, C. Gmachl, D. L. Sivco, J. N. Baillargeon, A. L. Hutchinson, A. Y. Cho, and H. C. Liu, "Self-mode-locking of quantum cascade lasers with giant ultrafast optical nonlinearities," Science **290**, 1739-1742 (2000).
13. F. Canbaz, I. Yorulmaz, and A. Sennaroglu, "Kerr-lens mode-locked 2.3-μm Tm^{3+}:YLF laser as a source of femtosecond pulses in the mid-infrared," Optics Letters **42**, 3964-3967 (2017).
14. J. Zhang, K. F. Mak, and O. Pronin, "Kerr-Lens Mode-Locked 2-μm Thin-Disk Lasers " IEEE Journal Selected Topic in Quantum Electronics **24**, 1-11 (2018).
15. M. Tokurakawa, E. Fujita, and C. Kränkel, "Kerr-lens mode-locked Tm^{3+}:Sc_2O_3 single-crystal laser in-band pumped by an Er:Yb fiber MOPA at 1611 nm," Optics Letters **42**, 3185-3188 (2017).
16. W. B. Cho, A. Schmidt, J. H. Yim, S. Y. Choi, S. Lee, F. Rotermund, U. Griebner, G. Steinmeyer, V. Petrov, X. Mateos, M. C. Pujol, J. J. Carvajal, M. Aguilo, and F. Diaz, "Passive mode-locking of a Tm-doped bulk laser near 2 μm using a carbon nanotube saturable absorber," Optics Express **17**, 11007-11012 (2009).
17. A. Suzuki, C. Kränkel, and M. Tokurakawa, "High quality-factor Kerr-lens mode-locked Tm:Sc_2O_3 single crystal laser with anomalous spectral broadening," Applied Physics Express **13**, 052007 (2020).
18. L. Wang, W. Chen, Y. Zhao, Y. Wang, Z. Pan, H. Lin, G. Zhang, L. Zhang, Z. Lin, and J. Bae, T. G. Park, F. Rotermund, P. Loiko, X. Mateos, M. Mero, U. Griebner and V. Petorv, "Single-walled carbon-nanotube saturable absorber assisted Kerr-lens mode-locked Tm:$MgWO_4$ laser," Optics Letters **45**, 6142-6145 (2020).
19. C. Kränkel, "Rare-Earth-Doped Sesquioxides for Diode-Pumped High-Power Lasers in the 1-, 2-, and 3-μm Spectral Range," IEEE Journal of Selected Topic in Quantum Electronics **21** (2015).
20. W. Jing, P. Loiko, J. M. Serres, Y. Wang, E. Vilejshikova, M. Aguiló, F. Díaz, U. Griebner, H. Huang, V. Petrov, and X. Mateos, "Synthesis, spectroscopy, and efficient laser operation of "mixed" sesquioxide Tm:(Lu,Sc)2O3 transparent ceramics," Optical Materials Express **7**, 4192-4202 (2017).
21. D. E. Zelmon, J. M. Northridge, N. D. Haynes, D. Perlov, and K. Petermann, "Temperature-dependent Sellmeier equations for rare-earth sesquioxides," Applied Optics **52**, 3824-3828 (2013).
22. P. Loiko, Y. C. Wang, J. M. Serres, X. Mateos, M. Aguilo, F. Diaz, L. Z. Zhang, Z. B. Lin, H. F. Lin, G. Zhang, E. Vilejshikova, E. Dunina, A. Kornienko, L. Fomicheva, V. Petrov, U. Griebner, and W. D. Chen, "Monoclinic Tm:$MgWO_4$ crystal: Crystal-field analysis, tunable and vibronic laser demonstration," Journal of Alloys and Compounds **763**, 581-591 (2018).
23. P. Loiko, X. Mateos, S. Y. Choi, F. Rotermund, J. M. Serres, M. Aguiló, F. Díaz, K. Yumashev, U. Griebner, and V. Petrov, "Vibronic thulium laser at 2131 nm Q-switched by single-walled carbon nanotubes," Journal of the Optical Society of America B **33**, D19-D27 (2016).